Journal of Power Sources 194 (2009) 1142–1149

Contents lists available at ScienceDirect

Journal of Power Sources

journal homepage: www.elsevier.com/locate/jpowsour

Solid-state hybrid photovoltaic cells with a novel redox polymer and nanostructured inorganic semiconductors

Zengfang Feng, Jianzhang Zhou, Yanyan Xi, Bibo Lan, Honghui Guo, Hongxiang Chen, Qiaobao Zhang, Zhonghua Lin*

State Key Laboratory of Physical Chemistry of Solid Surfaces and Department of Chemistry, College of Chemistry and Chemical Engineering, Xiamen University, Xiamen 361005, PR China

ARTICLE INFO

Article history:
Received 14 December 2008
Received in revised form 16 March 2009
Accepted 16 June 2009
Available online 24 June 2009

Keywords:
Photovoltaic cell
ZnO nanorod
CdSe
Redox polymer
Nafion

ABSTRACT

Here we introduce a new kind of stable inorganic/organic hybrid photovoltaic cells with redox polymers and nanostructured inorganic semiconductors. The redox polymers based on Nafion and metal complexes ($Ru(bpy)_3^{2+/3+}$ or $Fe(bpy)_3^{2+/3+}$) are applied in photovoltaic cells for the first time. These redox polymers with good charge transport performance are the hole transport material and the solid-state electrolyte in the photovoltaic cells. The nanoscale structures of inorganic semiconductors of ZnO nanorods/CdSe nanoparticle films used as the light-harvesting material are easily realized by a two-step electrodeposition. In terms of the preliminary current–voltage characterizations of the complete photovoltaic device (SnO_2:F/ZnO nanorods/CdSe/Nafion[$Ru(bpy)_3^{2+/3+}$, PEG]/Au), an overall energy conversion efficiency (() about 4% is achieved. A comparable energy conversion efficiency is also obtained for the photovoltaic cell with inexpensive $Fe(bpy)_3^{2+/3+}$ in the redox polymer. These photovoltaic cells retain 90% for their energy conversion efficiency in the first six months, showing the extended high stability. In addition, this kind of photovoltaic cells recovered easily by water due to the advantages of the Nafion-based redox polymer. These good results, joining with the easily accessible techniques of the cell fabrication, indicate that the proposed solid-state photovoltaic cells are hopefully to be a new type of 'cheap' and long-life photovoltaic devices for practical applications.

1. Introduction

As an alternative and clean energy source, photovoltaic cells have attracted great scientific and technological interest and have been extensively investigated in the past decades. Several new designs for photovoltaic devices [1–5] have been proposed. The representative dye-sensitized solar cells (DSSCs) [1] were considered as the third generation photovoltaic device, which may combine high-energy conversion efficiency with low production cost. Many impressive results have been obtained [6–8]. However, the composition of a stable and efficient electrolyte, along with a highly efficient and cost-effective light-harvesting material, remains the key parameters limiting the lifetime of photovoltaic cells and preventing them for further practical applications.

So far, great efforts have been made to replace the liquid electrolytes with quasi-solid-state or solid-state electrolytes, such as room-temperature ionic liquids [9,10], polymer gel [11–13], organic [14–16] and inorganic [17–19] hole transport materials. Each of these materials performs a specific task toward the overall objective of the energy conversion. Conducting polymers are well known as good charge transport materials. As conducting polymer electrolytes [20,21] can substitute the glass electrodes to improve the flexibility and to reduce resistances of solar cells, they might become a kind of competitive hole transport materials in photovoltaic devices. Regrettably, the conversion efficiencies of the cells employing conducting polymers [22–24] are lower in comparison to the cells using liquid or other polymer electrolytes. It is mainly due to the low conductivity and the low hole mobility of the conducting polymers, and the high charge recombination rate hereby.

Redox polymers are a kind of conducting polymers with advantages including simple preparation, high stability and good charge transport performance. Their applications have been widely investigated in catalysis [25], electrocatalysis [26], biosensors [27] and electrochemical supercapacitors [28]. However, it has not been reported for their application in photovoltaic cells. Here, the redox polymers based on Nafion [28–30] (a series of fluorinated sulfonic acid copolymers) and metal complexes ($Ru(bpy)_3^{2+/3+}$ or $Fe(bpy)_3^{2+/3+}$, bpy: 2,2′-bipyridine) were fabricated and applied in photovoltaic cells. In the photovoltaic cells, the metal complexes in the redox polymers capture the separated photo-generated carriers and then transmit the charges toward the counter electrode.

* Corresponding author. Tel.: +86 592 2189663; fax: +86 592 2189663.
E-mail address: zhlin@xmu.edu.cn (Z. Lin).

0378-7753/$ – see front matter.
doi:10.1016/j.jpowsour.2009.06.049

The redox polymers act as the hole transport material and the solid-state electrolyte of the photovoltaic cells. The charge transport mechanism [31,32] of the redox polymers may be the combination of physical diffusion (physical replacement) and charge hopping between redox centers. This mechanism is different from that of the solid-state electrolytes in which overall charge transport depends on ionic motions in the solid phase, and may result in higher charge transport rate of the redox polymer [28]. The higher charge transport rate is beneficial to the separation of the photo-generated electron–hole pairs and the transport of the carriers.

Organic materials used as the light-harvesting materials in photovoltaic cells exhibit great potential [33,34] due to the advantage of easy processing. However, the spectrally narrow absorption, low carrier mobility and fast aging of organic materials directly limit to achieve commercially viable device efficiency. Nanostructured inorganic semiconductors with appropriate bandgap (E_g, 1–2 eV) and high absorption coefficiency offer several advantages over organic materials [35], for example, the extended stability, the large surface area, the easily controllable synthesis and the relatively high intrinsic carrier mobility. Therefore, nanostructured inorganic semiconductors are probably the most promising light-harvesting materials for stable and efficient photovoltaic cells.

Consequently, a new type of solid-state hybrid photovoltaic cells with nanostructured inorganic semiconductors and redox polymer was proposed. And the photovoltaic cells with the structure of SnO_2:F conducting glass substrate/ZnO nanorods/CdSe/redox polymer (Nafion[$Ru(bpy)_3^{2+/3+}$ or $Fe(bpy)_3^{2+/3+}$, PEG])/Au were fabricated. The electrodeposited ZnO nanorods/CdSe nanoparticle films were used as the light-harvesting material. Their morphology, structural and optical properties were recorded and analyzed. The solid-state Nafion[$Ru(bpy)_3^{2+/3+}$ or $Fe(bpy)_3^{2+/3+}$, PEG] redox polymer films were prepared and then their charge transport performances were studied by electrochemical methods. The photocurrent spectra and current–voltage (J–V) measurements of the complete photovoltaic cells were carried out. The influence of the thickness of CdSe nanopaticles layer on the performance of these photovoltaic cells was studied, and the stability with time was evaluated.

2. Experimental

2.1. ZnO nanorods/CdSe electrodeposition

ZnO nanorods were prepared by the method of potentiostatic cathodic reduction based on the work of Cui and Gibson [36]. The electrodeposition was carried out in a three-electrode system, in which Pt foil worked as the counter electrode, a saturated calomel electrode (SCE) served as reference electrode, and the fore-treated SnO_2:F conducting glass substrate (14 Ω q^{-1}, Ashi Company, 1 cm × 3 cm) was used as the working electrode. The deposition was in the electrolyte of $Zn(NO_3)_2$ (5 mM, Alfa Aesar) and hexamethylenetetramine (5 mM, Alfa Aesar) aqueous solution and under potentiostatic condition of −0.9 V (vs. SCE) for 50 min using a Potentiostat/Galovanostat (Model 173, EG&G, PAR.). The bath temperature was 90 °C. The charge density used in the ZnO electrodeposition of all the samples in this work was 0.6 C cm^{-2}.

The cathodic electrodeposition [37] of CdSe coating ZnO nanorods was carried out galvanostatically from a constant stirring bath containing $CdCl_2$ (10 g L^{-1}, Alfa Aesar) and saturated solution of Se in dimethylformamide (DMF, non-aqueous). The current density was 0.22 mA cm^{-2}. With different time of deposition, CdSe layers were of different thicknesses. The temperature of the deposition bath was 125 °C. The photoelectrodes of ZnO nanorods/CdSe were annealed under the temperature of 350 °C for 60 min.

2.2. Preparation and characterization of the solid-state redox polymer film

The redox polymer film was prepared by the method introduced by Bard [31] and Kobayashi [32]. Nafion solution (1 g, DuPont, DE1020) blended with polyethylene glycol (PEG, 25 mg, Alfa Aesar), was spin-coated on the photoelectrodes (ZnO nanorods/CdSe) to form a Nafion film. Then the Nafion film was dipped into the saturated solution of $Ru(bpy)_3^{2+/3+}$ or $Fe(bpy)_3^{2+/3+}$. The solid-state Nafion[$Ru(bpy)_3^{2+/3+}$ or $Fe(bpy)_3^{2+/3+}$, PEG] redox polymer based on Nafion and metal complex were formed through the ion-exchange reaction of $Ru(bpy)_3^{2+}$ and H^+ in Nafion. After dried in a glass desiccator for one week, the thickness of the solid-state Nafion film measured with a Dektak3 Series Elcometer was about 10 μm, and the total concentration of H^+ sites was 1 mol L^{-1}.

To investigate the charge transport performances of the solid-state Nafion[$Ru(bpy)_3^{2+/3+}$, PEG] redox polymer, some sandwich-type devices of SnO_2:F/Nafion[$Ru(bpy)_3^{2+/3+}$, PEG]/Au were first constructed. Then cyclic voltammetry (CV) [38] and electrochemical impedance spectroscopy (EIS) [39] were introduced to study the charge transport performance. As further investigation, we studied the charge transport performance of the redox polymers with or without PEG, and found the optimal PEG content. The experiments were carried out after the sandwich-type devices of SnO_2:F/Nafion[$Ru(bpy)_3^{2+/3+}$, PEG]/Au dried in a glass desiccator for ten days, to ensure that the results can reflect the real charge transport behavior in the 'dry' redox polymer films of the solid-state photovoltaic cells. The Au film with the thickness about 300 nm was sputtered as the counter electrode of the devices.

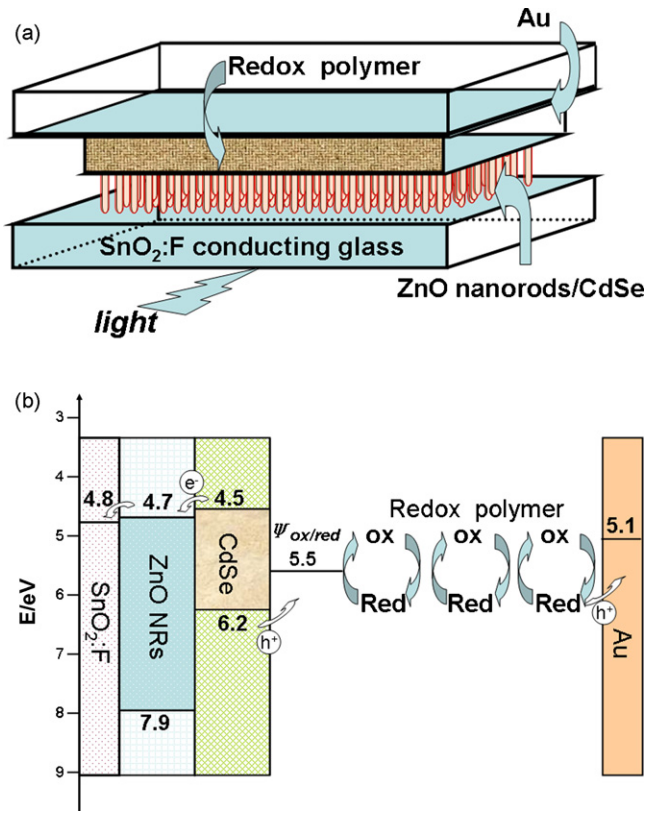

Fig. 1. The structure (a) and the energy diagram (b) of the solid-state photovoltaic cell SnO_2:F/ZnO nanorods/CdSe/Redox polymer/Au. Redox polymer: Nafion[$Ru(bpy)_3^{2+/3+}$ or $Fe(bpy)_3^{2+/3+}$, PEG], in Fig. 1b, we take the $\psi_{ox/red}$ = 5.5 eV (1.1 V) of $Ru(bpy)_3^{2+/3+}$ for example.

2.3. Cell assembly

Fig. 1 shows the structure (a) and the energy diagram (b) of the solid-state photovoltaic cells of SnO_2:F/ZnO nanorods/CdSe/Redox polymer/Au. Here, the CdSe nanoparticles layer coating ZnO nanorods (NRs) on SnO_2:F conducting glass substrate was used as a composite photoanode. The ZnO nanorods layer was used as transparent window and electron transport material due to its proper bandgap and high carrier mobility. The redox polymer of Nafion and metal complexes ($Ru(bpy)_3^{2+/3+}$ or $Fe(bpy)_3^{2+/3+}$) was used as the solid-state hole transport material in the photovoltaic cells. In order to avoid short circuit in the cell, the Au film with the thickness about 300 nm was sputtered onto another piece of SnO_2:F conducting glass substrate as counter electrode.

As shown in Fig. 1b, the work functions of 4.8 eV for the F-doping SnO_2 conducting glass and 5.1 eV for the Au cathode are determined from the ultra-violet photoemission spectra (UPS) [40]. And the energy values of ZnO and CdSe are determined from their cyclic voltammetry [41,42] and UV–Vis absorption spectra (the experiment details of UPS and cyclic voltammetry are shown in ESI). The offset between the CdSe VB and the Au work function is 1.1 eV (Fig. 1b), which will be conducive to the hole transport from CdSe to the Au cathode. The matching between the energy band structure of ZnO and CdSe will facilitate the separation of the photo-generated electron–hole pairs.

2.4. Measurements

The photocurrent action spectra and current–voltage (*J–V*) characterizations of the cells were obtained with a photoelectrochemical measurement system, which was consisted of a potentiostat (Model 273, EG&G, PAR.), a two phase lock-in amplifier (Model 5206, EG&G, PAR.) with a chopper (Model 194A, EG&G, PAR.). The white light illumination of 25 mW cm^{-2} (1/4 sun) was from a Xenon lamp of 150 W, and the active area of the cell was 0.10 cm^2. A solar simulator (Class B, Model 91160, NEWPORT, USA) with a 300 W Xenon lamp and a Air Mass 1.5 filter provided the white light illumination of 100 mW cm^{-2}. The incident light power was calibrated using an RK-5710 power radiometer (Laser Probe Inc.). The results were not further corrected with respect to transmission losses in the conducting substrate. Monochromatic light was obtained in the range of 300–800 nm using a SpectraPro 275 Monochromator (Acton Research Corporation). The absorption spectra were recorded by a Varian Cary 5000 UV–Vis–NIR spectrometer and the scanning electron microscope (SEM) images were recorded by LEO-1530. Finally, electrochemical experiments

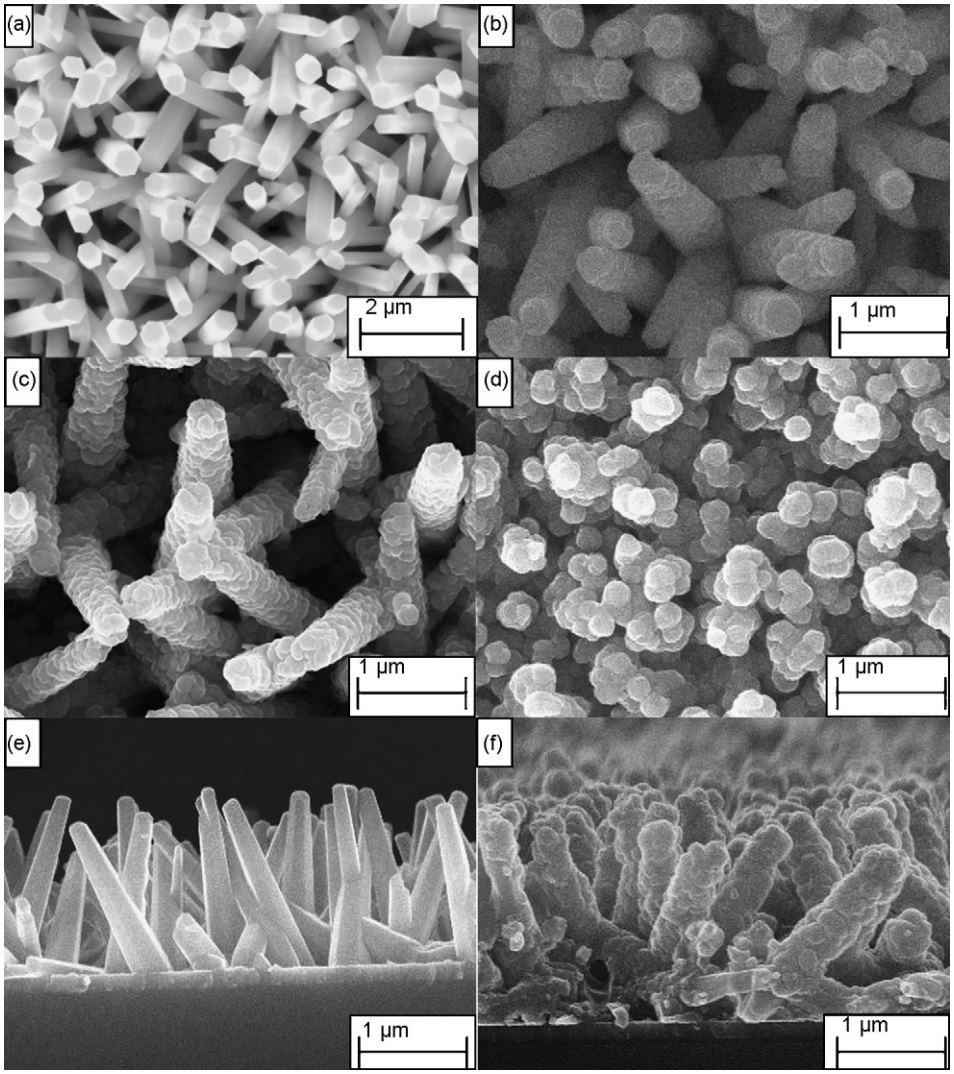

Fig. 2. Scanning electron microscopy (SEM) images. Top view: (a) ZnO nanorods, (b) ZnO nanorods/CdSe, the charge amount used in CdSe electrodeposition is 0.1 C cm^{-2}, (c) ZnO nanorods/CdSe, the charge amount used in CdSe electrodeposition is 0.2 C cm^{-2}, (d) ZnO nanorods/CdSe, the charge used in CdSe electrodeposition is 0.5 C cm^{-2}, cross section: (e) ZnO nanorods, (f) ZnO nanorods/CdSe, the charge amount used in CdSe electrodeposition is 0.2 C cm^{-2}.

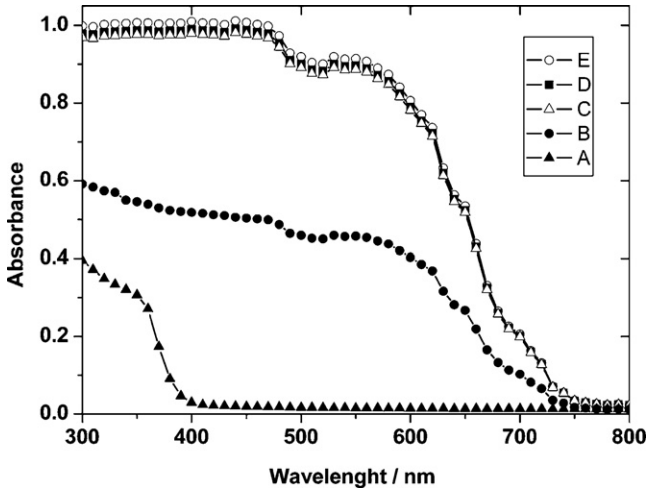

Fig. 3. The absorption spectra of the samples. A: SnO_2:F/ZnO nanorods, B: SnO_2:F/ZnO nanorods/CdSe, the charge amount used in CdSe electrodeposition was 0.1 C cm^{-2}. C: SnO_2:F/CdSe, the charge amount used in CdSe electrodeposition was 0.2 C cm^{-2}. D: SnO_2:F/ZnO nanorods/CdSe, the charge amount used in CdSe electrodeposition was 0.2 C cm^{-2}. E: SnO_2:F/ZnO nanorods/CdSe, the charge amount used in CdSe electrodeposition was 0.5 C cm^{-2}.

were carried out using computer controlled electrochemical workstations (Model 630, CH Instruments, USA and Model PGSTAT12, Autolab, Metrohm AG). All the experiments were carried out in room temperature (25 °C).

3. Results and discussion

3.1. Morphology

As can be seen in the SEM images of Fig. 2a and e, the ZnO nanorods exist a notable roughness, attributed to the rough surface of SnO_2:F conducting glass substrates. The height of the ZnO nanorods increases with the charge amount used in ZnO electrodeposition. Meanwhile, their diameter remains approximately a constant. For the charge of 0.6 C cm^{-2} used in ZnO electrodeposition, the height of the nanorod is close to 1.5 μm and the diameter is within the range of 150–250 nm. Considering the average surface area (1.5 μm in height and 200 nm in diameter) of $\sim 1 \times 10^{-8}$ cm^2 and the typical density of $\sim 1.5 \times 10^9$ cm^{-2} nanorods, a surface enlargement factor close to 15 can be estimated for these ZnO nanorods samples. This surface enlargement is beneficial to the light harvesting and the photon-generation, which will mention afterwards.

As shown in Fig. 2b, c, and f, the electrodeposited CdSe nanoparticles spread on the surface of ZnO nanorods and form a layer of CdSe nanoparticles. The thickness of the CdSe nanoparticles layer increases with the charge used in CdSe electrodeposition. With the used charge of 0.1 and 0.2 C cm^{-2}, the thicknesses of CdSe layer (around the ZnO nanorods) are respectively in the ranges of 20–30 nm and 40–50 nm, which were estimated from a statistical evaluation of the nanorod diameters before and after the CdSe deposition. With a larger charge (0.5 C cm^{-2}) in electrodeposition, the CdSe nanoparticles full-fill the interspace of the ZnO nanorods and form a dense CdSe film (Fig. 2d).

3.2. Optical properties

The UV–Vis absorption spectra of the SnO_2:F/ZnO nanorods, SnO_2:F/CdSe and SnO_2:F/ZnO nanorods/CdSe samples are shown in Fig. 3. The energy gap (E_g) of different semiconductor layers was estimated by using the relation to the direct optical transition [43]:

$$E_g(\text{eV}) \approx 1240/\lambda_e\,(\text{nm})$$

where λ_e is the absorption onset. The E_g of 3.14 eV for ZnO nanorods and 1.68 eV for CdSe nanoparticles are calculated with the absorption onsets of 395 nm and 740 nm from the absorption spectra, respectively. Both values were in good correlation with previously reported values [44,45]. The coherence of the absorption spectra for SnO_2:F/ZnO nanorods/CdSe and SnO_2:F/CdSe (with and without the ZnO nanorods) indicated that ZnO nanorods contributed little in the light-trapping procedure for the cells. In comparison of the absorption spectra of the SnO_2:F/ZnO nanorods/CdSe samples with different charge densities used in CdSe electrodeposition, we thought that the light absorption was insufficient for the sample with the charge density 0.1 C cm^{-2} used in the CdSe electrodeposition. As shown in Fig. 3, the absorption spectrum of SnO_2:F/ZnO nanorods/CdSe sample was in good correlation with the solar spectrum, which indicated that ZnO nanorods/CdSe was appropriate to be a light-harvesting material.

As it is well known, in addition to acting as charge carriers, the metal complexes of $Ru(bpy)_3^{2+/3+}$ and $Fe(bpy)_3^{2+/3+}$ themselves are also photoactive. In the comparison of the UV–Vis absorption spectra (shown in supplementary information) of SnO_2:F/ZnO nanorods/CdSe and SnO_2:F/ZnO nanorods/CdSe/Nafion[$Ru(bpy)_3^{2+/3+}$ or $Fe(bpy)_3^{2+/3+}$, PEG] samples, the metal complexes contribute little to the light absorption. Additionally, the metal complexes were fixed in Nafion the redox polymer films. Therefore, the metal complexes of $Ru(bpy)_3^{2+/3+}$ and $Fe(bpy)_3^{2+/3+}$ under illumination just act as charge transport materials in the redox polymer.

Table 1
The details of D_{ct} and μ of solid-state redox polymers with different complexes and concentration.

Methods	Charge transport process	C_0 (10^{-5} mol L^{-1})	D_{ct} (10^{-5} cm^2 s^{-1})	μ (10^{-4} cm^2 V^{-1} s^{-1})
CV	$Ru(bpy)_3^{2+} \rightarrow Ru(bpy)_3^{3+}$	1.52 ± 0.05	0.65 ± 0.02	2.60 ± 0.09
		5.0 ± 0.2	1.74 ± 0.06	7.0 ± 0.3
	$Ru(bpy)_3^{3+} \rightarrow Ru(bpy)_3^{2+}$	1.52 ± 0.05	0.61 ± 0.02	2.45 ± 0.08
		5.0 ± 0.2	1.65 ± 0.05	6.6 ± 0.2
	$Fe(bpy)_3^{2+} \rightarrow Fe(bpy)_3^{3+}$	1.78 ± 0.06	0.60 ± 0.02	2.40 ± 0.08
		5.6 ± 0.2	1.62 ± 0.05	6.5 ± 0.2
	$Fe(bpy)_3^{3+} \rightarrow Fe(bpy)_3^{2+}$	1.78 ± 0.06	0.56 ± 0.02	2.25 ± 0.08
		5.6 ± 0.2	1.57 ± 0.05	6.3 ± 0.2
EIS	$Ru(bpy)_3^{2+} \leftrightarrow Ru(bpy)_3^{3+}$	1.52 ± 0.06	0.70 ± 0.02	2.81 ± 0.09
		5.0 ± 0.2	2.11 ± 0.07	8.4 ± 0.3
	$Fe(bpy)_3^{2+} \leftrightarrow Fe(bpy)_3^{3+}$	1.78 ± 0.07	0.64 ± 0.02	2.55 ± 0.09
		5.6 ± 0.2	1.69 ± 0.06	6.8 ± 0.3

C_0: the concentration of the metal complexes, D_{ct}: the apparent charge transport diffusion coefficient and μ: the charge carrier mobility. The relative standard deviations (RSD) are 3–4%.

Table 2
The charge transport performances of the redox polymer with various PEG contents. The calculated concentrations of the redox molecules ($Ru(bpy)_3^{2+/3+}$) in these samples are about 1.52×10^{-5} mol L^{-1}.

PEG contents/mg g^{-1}	0	5	15	25	35	45
D_{ct} (cm^2 s^{-1})	8.13×10^{-7}	1.35×10^{-6}	4.02×10^{-6}	6.50×10^{-6}	4.21×10^{-6}	2.16×10^{-6}
μ (cm^2 V^{-1} s^{-1})	3.25×10^{-5}	5.4×10^{-5}	1.61×10^{-4}	2.60×10^{-4}	1.68×10^{-4}	8.64×10^{-5}

3.3. The charge transport performance of the solid-state redox polymer films

There are two factors that may influence the charge transport performance of the solid redox polymer: the microstructure of the Nafion films on the one hand [28,32], and the concentration of the redox molecules (the metal complexes) in the polymer on the other hand. For the low solubility of $Ru(bpy)_3^{2+}$, the amount of redox molecules exchanged into the Nafion film is low, as well as the concentration of redox molecules in the solid-state polymer film. The concentrations (C_0 in Table 1) of the redox molecules with electrochemical activity are calculated from the solid-state cyclic voltammetry [46] (the calculation details are also available in ESI). The maximum concentration is measured only about 10^{-4} mol L^{-1}. According to the CV and EIS experiments of the redox polymer with the SnO_2:F/Redox Polymer/Au devices, the apparent charge transport diffusion coefficient (D_{ct}) of 10^{-6} to 10^{-5} cm^2 s^{-1} and the charge carrier mobility (μ) about 10^{-4} cm^2 V^{-1} s^{-1} for the redox polymer Nafion[$Ru(bpy)_3^{2+/3+}$, PEG] were obtained (Table 1). The charge carrier mobilities (μ) were achieved according to the following Einstein's equation:

$$\mu/\mathrm{cm^2\,s^{-1}\,V^{-1}} = \frac{e}{KT} D_{ct} \approx 40 D_{ct}/\mathrm{cm^2\,s^{-1}} (298\,\mathrm{K})$$

where e is the elementary charge of electron, K is the Boltzmann constant, and T is absolute temperature.

The addition of PEG can improve the conductivity of redox polymer films [32] by the effect of the microstructure of the redox polymer. We have investigated the charge transport performances of the solid-state redox polymer with various PEG contents. The redox polymer with PEG content of 25 mg g^{-1} represents the best charge transport performances (Table 2). In addition, the I–V curves for SnO_2:F/Redox Polymer/Au devices with or without PEG in the redox polymer are shown in Fig. 4. The ratio for the current densities of the redox polymers with or without PEG at ±2 V is approximately 10, showing the good rectification efficiency of the redox polymers with PEG. The similar results can be obtained with the redox polymer using $Fe(bpy)_3^{2+/3+}$ as the redox molecules.

The redox polymers exhibit the comparable charge transport performance with the organic hole transport materials [16,31]. Furthermore, the charge transport performance of Nafion[$Fe(bpy)_3^{2+/3+}$, PEG] (with $Fe(bpy)_3^{2+/3+}$ as the redox molecules) has also been studied. The results showed that it had high charge transport performance compared with Nafion[$Ru(bpy)_3^{2+/3+}$, PEG]. Therefore, Nafion[$Fe(bpy)_3^{2+/3+}$, PEG] could be a potential candidate for the solid hole transport material in the solid-state photovoltaic cells, due to the much lower cost of $Fe(bpy)_3^{2+/3+}$ than $Ru(bpy)_3^{2+/3+}$.

3.4. Characterizations of the solid-state photovoltaic cells

The typical current–voltage (J–V) characteristics in dark and under the 25 mW cm^{-2} white light illumination of photovoltaic cell with the structure of SnO_2:F/ZnO nanorods/CdSe/Nafion[$Ru(bpy)_3^{2+/3+}$, PEG]/Au are shown in Fig. 5. The short-circuit current density (J_{sc}), open-circuit voltage (V_{oc}) and fill factor (FF) are 2.30 mA cm^{-2}, 553 mV and 0.74, respectively, and an overall energy conversion efficiency (() of 3.8% is achieved. The photocurrent action spectrum of the photovoltaic cell is shown in Fig. 6. The reflective loss of the complete cell was not taken into account in the incident photon-to-current conversion efficiency (IPCE) calculation. The IPCE of the cell exceeded 40% in a broad spectral range from 300 to 640 nm, reaching its maximum of 51% at 480 nm. This good correlation with the energy range of the solar spectral reconfirmed that CdSe was a suitable light-harvesting material.

A series of photovoltaic cells with different charge amounts used in the CdSe electrodeposition (i.e., the different thickness of CdSe nanoparticles layer) was fabricated and the current–voltage (J–V) characterizations were measured. The characteristic parameters of J_{sc}, V_{oc}, FF and (are summarized and shown in Fig. 7. The

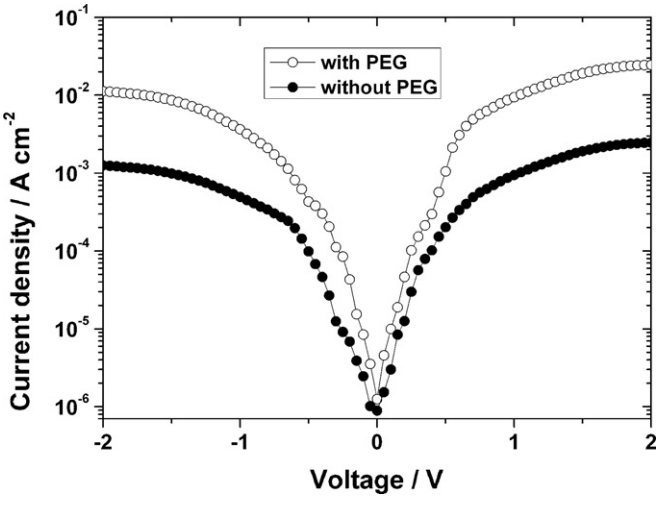

Fig. 4. I–V curves for SnO_2:F/Redox Polymer/Au with or without PEG in the redox polymer. The redox molecules: $Ru(bpy)_3^{2+/3+}$, PEG content: 25 mg g^{-1}.

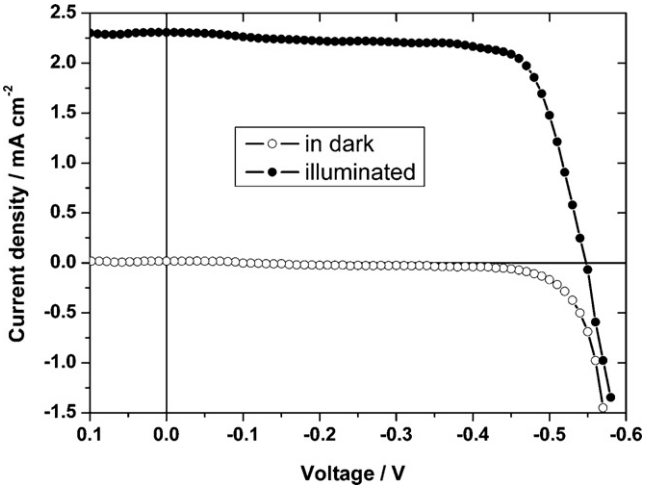

Fig. 5. The current–voltage (J–V) characteristic of a SnO_2:F/ZnO nanorods/CdSe/Nafion[$Ru(bpy)_3^{2+/3+}$, PEG]/Au photovoltaic cell. V_{oc} = 553 mV, J_{sc} = 2.30 mA cm^{-2}, FF = 0.74, (= 3.8% (in the 25 mW cm^{-2} white light illumination and the active area of 0.1 cm^2, J_{sc}: short-circuit current density, V_{oc}: open-circuit voltage, FF: fill factor, (: energy conversion efficiency).

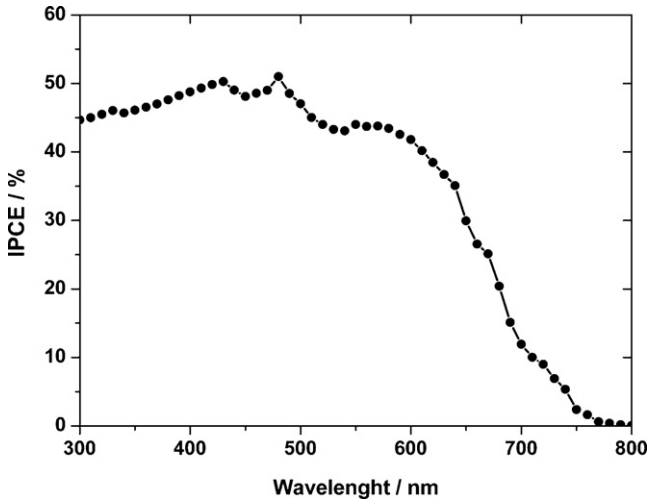

Fig. 6. The incident photon-to-current conversion efficiency (IPCE) spectrum of SnO_2:F/ZnO nanorods/CdSe/Nafion[$Ru(bpy)_3^{2+/3+}$, PEG]/Au photovoltaic cell (under short circuit).

photovoltaic cell with the charge amount in the CdSe electrodeposition of 0.2 C cm^{-2} represents the best performance. We can explain from the morphology (Fig. 2) and the UV–Vis absorption spectra (Fig. 3) as follows. As we know, the key points in improving the energy conversion efficiency of the photovoltaic cell are the increase of the photon-generated carriers and the efficient separation of electron–hole pairs, as well as their collection [16,47–49]. The increase of the photon-generated carriers strongly depends on the light absorption, which relies on the material of light-trapping layer and its adequate thickness. Meanwhile, the separation and collection efficiency of the photon-generated electron–hole pairs depend on the distance of the electron–hole pairs traveling over (i.e., the thickness of CdSe nanoparticle layer) and the interface area where the electron–hole pairs are separated and collected [50–52]. There are more recombinations during the electron–hole pairs traveling over long distance before being separated and collected, which will result in a reduction of J_{sc}, FF, and finally decrease the energy conversion efficiency. The thickness of CdSe nanoparticles layer with the charge density of 0.1 C cm^{-2} is only about 20–30 nm, which leads to the insufficient light absorption and a poor photoelectric performance. The notable surface enlargement of ZnO nanorods allows a reduction in the thickness of CdSe layer, which will significantly improve the collection efficiency of electron–hole pairs. The similar behavior has been observed in the extremely thin absorber (ETA) solar cells [50]. In addition, the scattering at the interfaces of ZnO nanorods/CdSe will increase the optical path through the sample and induce the enhancement of the photon absorption, which was known as the light-trapping effect [53]. With increasing the charge amount to 0.2 C cm^{-2} in the electrodeposition, the CdSe layer can harvest enough light. However, if the charge amount increases continuously in the electrodeposition (0.5 C cm^{-2} or even more) procedure, there are more recombinations during the electron–hole pairs traveling over large distances of the thicker CdSe layer. Therefore, the photovoltaic cell with the charge amount in CdSe electrodeposition of about 0.2 C cm^{-2} represents the best performance.

To study the stability of these solid-state photovoltaic cells, the aging tests of another series of current–voltage (*J–V*) characterizations with a same cell have been carried out. The time-dependent changes of the characteristic parameters are shown in Fig. 8. The energy conversion efficiencies measured as the cell was fabricated, 1 week later, 1 month later, 2 months later and 6 months later are 3.8%, 4.0%, 3.7%, 3.5%, 3.4%, respectively (The completed cell was stored in a transparent glass desiccator and under ambient light during this period). Attributed to the increase of J_{sc} and V_{oc}, the energy conversion efficiency moderately increases to 4.0% 1 week after fabrication. A similar phenomenon has been observed in solid-state DSSCs and ETA solar cells [50]. The cells retain 90% for its energy conversion efficiency over six months, showing the high stability of these photovoltaic cells.

The charge mobility of the Nafion[$Ru(bpy)_3^{2+/3+}$ or $Fe(bpy)_3^{2+/3+}$, PEG] redox polymer strongly depends on the microstructure of the redox polymer films [28,29,32]. The moisture in the redox polymer can ameliorate the microstructure of the redox polymer films to increase the charge mobility. It may play a role in enhancing the device efficiency. Consequently, after 6 months dried in the glass desiccator, the completed cell (the same cell as used in Fig. 8)

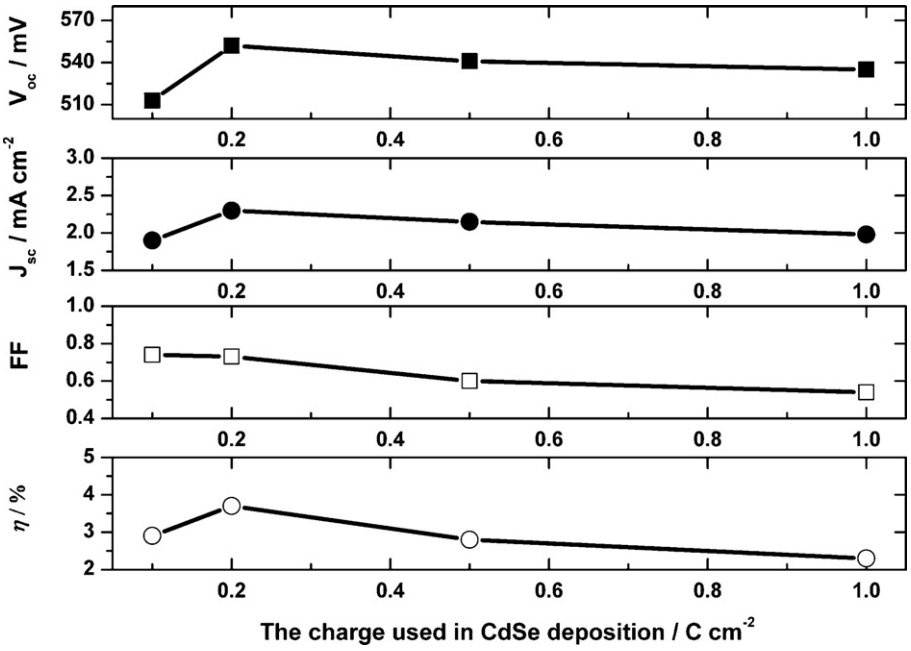

Fig. 7. Characteristic parameters of SnO_2:F/ZnO nanorods/CdSe/Nafion[$Ru(bpy)_3^{2+/3+}$, PEG]/Au photovoltaic cells with different charge used in CdSe deposition.

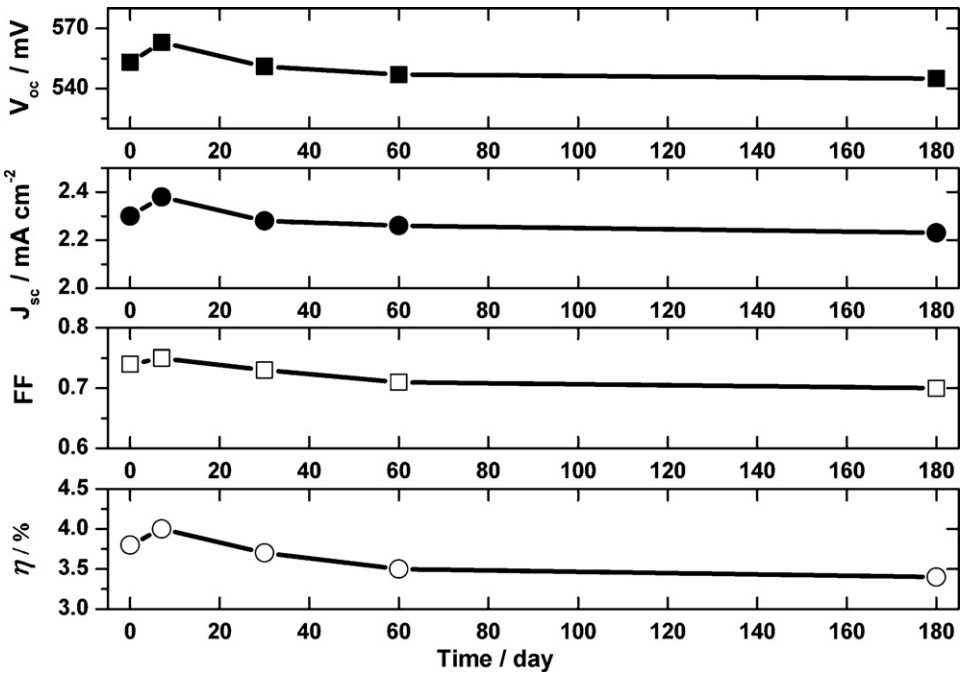

Fig. 8. Characteristic parameters of a same SnO_2:F/ZnO nanorods/CdSe/Nafion[$Ru(bpy)_3^{2+/3+}$, PEG]/Au photovoltaic cell measured at different time.

was kept in a moisture-saturated container for one week. And after that, we measured the *J–V* performance of the cell (The *J–V* curve shows in ESI). The J_{sc}, V_{oc}, and FF are 2.52 mA cm^{-2}, 558 mV and 0.74, respectively, yielding an overall energy conversion efficiency of 4.2%, which is even slightly higher than the initial value. The results imply that this kind of photovoltaic cells can be recovered easily by water. It is hopefully that these photovoltaic cells can be a kind of 'rejuvenatable' photovoltaic cells with long life.

Furthermore, the performance of the solid-state photovoltaic cell with $Fe(bpy)_3^{2+/3+}$ as redox molecules in the redox polymer was studied, intending to replace the relative high price $Ru(bpy)_3^{2+/3+}$. Fig. 9 shows the *J–V* curves in dark and under 25 mW cm^{-2} white light illumination of the photovoltaic cell of SnO_2:F/ZnO nanorods/CdSe/Nafion[$Fe(bpy)_3^{2+/3+}$, PEG]/Au. The J_{sc}, V_{oc}, FF are 2.22 mA cm^{-2}, 545 mV and 0.70, respectively, yielding an overall energy conversion efficiency of 3.4% which is comparable with the photovoltaic cell with $Ru(bpy)_3^{2+/3+}$ as metal complexes in the redox polymer. The results demonstrated that this kind of solid-state photovoltaic cells were promising to be practical photovoltaic devices with long-term stability, low production cost and high-energy conversion efficiency.

Finally, to study the light intensity on the photovoltaic cell, we evaluated the photovoltaic cells under the various white light illuminations of 25 mW cm^{-2}, 50 mW cm^{-2}, 75 mW cm^{-2} and 100 mW cm^{-2}, respectively. These white light illuminations are from a solar simulator with a 300 W Xenon lamp and a Air Mass 1.5 filter. As shown in Fig. 10, with the incident light power intensity increase, the short-circuit current density (J_{sc}) increase from 2.37 mA cm^{-2} to 9.08 mA cm^{-2}, meanwhile only a slightly increase of 12 mV for the open-circuit voltage (V_{oc}), the fill factors almost keep a constant about 0.74, and the overall energy conversion efficiencies (() are near, in the range of 3.8–4.1%. We evaluated some

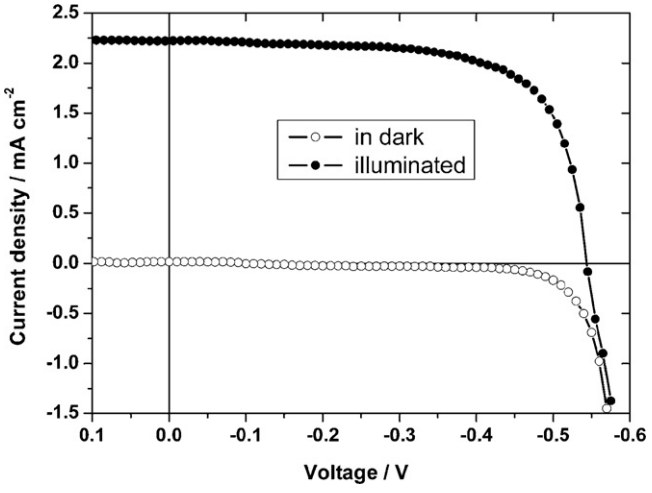

Fig. 9. The current–voltage (*J–V*) characteristics of SnO_2:F/ZnO nanorods/CdSe/Nafion[$Fe(bpy)_3^{2+/3+}$, PEG]/Au photovoltaic cell. V_{oc} = 545 mV, J_{sc} = 2.22 mA cm^{-2}, FF = 0.70, (= 3.4% (in the 25 mW cm^{-2} white light illumination and the active area of 0.1 cm^2).

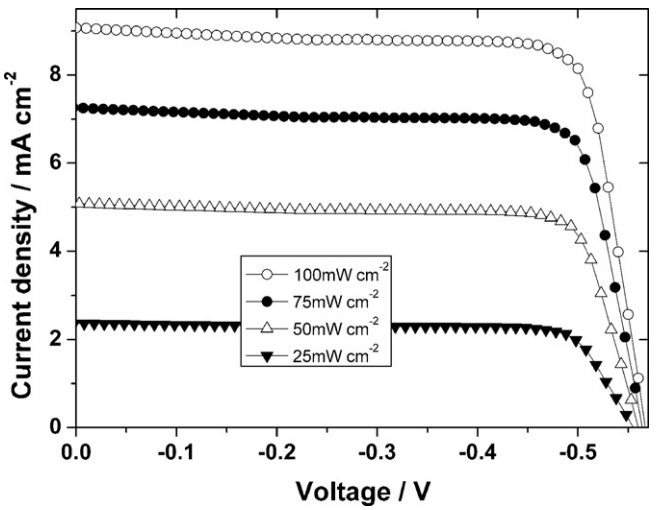

Fig. 10. The current–voltage (*J–V*) characteristics under various incident light intensities of 25 mW cm^{-2}, 50 mW cm^{-2}, 75 mW cm^{-2} and 100 mW cm^{-2}, respectively. The cell structure: SnO_2:F/ZnO nanorods/CdSe/Nafion[$Ru(bpy)_3^{2+/3+}$, PEG]/Au.

other cells under the white light illumination of 100 mW cm^{-2} (AM1.5), with the standardized characteristic parameters shows in ESI.

4. Conclusions

We elucidated a photovoltaic device which utilizes the popular semiconductors of ZnO nanorods/CdSe as light-harvesting materials and redox polymers Nafion[Ru(bpy)$_3$$^{2+/3+}$ or Fe(bpy)$_3$$^{2+/3+}$, PEG] as the charge transport materials. The nanostructured inorganic semiconductor of ZnO nanorods/CdSe represented good performance in light trapping. The solid-state redox polymers of Nafion[Ru(bpy)$_3$$^{2+/3+}$ or Fe(bpy)$_3$$^{2+/3+}$, PEG] with high charge transport performance are promising to be a new type hole transport material in photovoltaic cells. The good results primarily achieved were comparable with those of ETA solar cells which used the similar inorganic semiconductor materials [46,47] and the DSSCs with other conducting polymer electrolytes [22–24]. Furthermore, with the optimization of the techniques in fabricating, for example, the high-density vertically aligned ZnO nanorods, the optimum of the redox polymer film, these solid-state photovoltaic cells are of considerable potential for practical application due to the long-term stability, easy fabricating and low cost.

Acknowledgements

We are grateful to the support of the National Nature Science Foundation of China (grant Nos. 20433040 and 20373057). Thanks very much for the helpful discussions with Prof. Deyin Wu and Prof. Nanfeng Zheng.

Appendix A. Supplementary data

Supplementary data associated with this article can be found, in the online version, at doi:10.1016/j.jpowsour.2009.06.049.

References

[1] B. O'Regan, M. Grätzel, Nature 353 (1991) 737–739.
[2] G. Yu, J. Gao, J.C. Hummelen, F. Wudl, A.J. Heeger, Science 270 (1995) 1789–1791.
[3] R. Könenkamp, P. Hoyer, A. Wahi, J. Appl. Phys. 79 (1996) 7029–7035.
[4] A.J. Nozik, Physica E 14 (2002) 115–120.
[5] J. Xue, B.P. Rand, S. Uchida, S.R. Forrest, Adv. Mater. 17 (2005) 66–71.
[6] Y. Bai, Y.M. Cao, J. Zhang, M.K. Wang, R.Z. Li, P. Wang, S.M. Zakeeruddin, M. Grätzel, Nat. Mater. 7 (2008) 626–630.
[7] Y. Chiba, A. Islam, Y. Watanabe, R. Komiya, N. Koide, L. Han, Jpn. J. Appl. Phys. 45 (2006) L638–L640.
[8] L. Schmidt-Mende, U. Bach, R. Humphry-Baker, T. Horiuchi, H. Miura, S. Ito, S. Uchida, M. Grätzel, Adv. Mater. 17 (2005) 813–815.
[9] W. Kubo, T. Kitamura, K. Hanabusa, Y. Wada, S. Yanagida, Chem. Commun. 2 (2002) 374–375.
[10] P. Wang, B. Wenger, R. Humphry-Baker, J.E. Moser, J. Teuscher, W. Kantlehner, J. Mezger, E.V. Stoyanov, S.M. Zakeeruddin, M. Grätzel, J. Am. Chem. Soc. 127 (2005) 6850–6856.
[11] A.F. Nogueira, J.R. Durrant, M.A. De Paoli, Adv. Mater. 13 (2001) 826–830.
[12] P. Wang, S.M. Zakeeruddin, J.E. Moser, M.K. Nazeeruddin, T. Sekiguchi, M. Grätzel, Nat. Mater. 2 (2003) 402–407.
[13] X. Zhang, H. Yang, H.M. Xiong, F.Y. Li, Y.Y. Xia, J. Power Sources 165 (2007) 911–915.
[14] J. Hagen, W. Schaffrath, P. Otschik, R. Fink, A. Bacher, H.-W. Schmidt, D. Haarer, Synth. Met. 89 (1997) 215–220.
[15] U. Bach, D. Lupo, P. Comte, J.E. Moser, F. Weissörtel, J. Salbeck, H. Spreitzer, M. Grätzel, Nature 395 (1998) 583–585.
[16] J. Krüger, R. Plass, L. Cevey, M. Piccireli, M. Grätzel, U. Bach, Appl. Phys. Lett. 79 (2001) 2085–2087.
[17] L. Schmidt-Mende, A. Fechtenkötter, K. Müllen, E. Moons, R.H. Friend, J.D. MacKenzie, Science 293 (2001) 1119–1122.
[18] G.R.A. Kumara, A. Konno, K. Shiratsuchi, J. Tsukahara, K. Tennakone, Chem. Mater. 14 (2002) 954–955.
[19] B.C. O'Regan, S. Scully, A.C. Mayer, E. Palomares, J. Durrant, J. Phys. Chem. B 109 (2005) 4616–4623.
[20] S. Günes, N.S. Sariciftci, Inorg. Chim. Acta 361 (2008) 581–588.
[21] A.F. Nogueira, C. Longo, M.A. De Paoli, Coord. Chem. Rev. 248 (2004) 1455–1468.
[22] S. Luzzati, M. Basso, M. Catellani, C.J. Brabec, D. Gebeyehu, N.S. Sariciftci, Thin Solid Films 403–404 (2002) 52–56.
[23] T.K. Däubler, I. Glowacki, U. Scherf, J. Ulanski, H.H. Hörhold, D. Neher, J. Appl. Phys. 86 (1999) 6915–6923.
[24] G.P. Smestad, S. Spiekermann, J. Kowalik, C.D. Grant, A.M. Schwartzberg, J. Zhang, L.M. Tolbert, E. Moons, Sol. Energy Mater. Sol. Cells 76 (2003) 85–105.
[25] M. Králik, A. Biffis, J. Mol. Catal. A: Chem. 177 (2001) 113–138.
[26] A. Malinauskas, Synth. Met. 107 (1999) 75–83.
[27] J. Wang, Chem. Rev. 108 (2008) 814–825.
[28] M. Kaneko, Prog. Polym. Sci. 26 (2001) 1101–1137.
[29] V. Neburchilov, J. Martin, H. Wang, J. Zhang, J. Power Sources 169 (2007) 221–238.
[30] K.A. Mauritz, R.B. Moore, Chem. Rev. 104 (2004) 4535–4586.
[31] I. Rubinstein, A.J. Bard, J. Am. Chem. Soc. 102 (1980) 6641–6642.
[32] N. Kobayashi, S. Miyamura, K. Teshima, R. Hirohashi, Electrochim. Acta 43 (1998) 1639–1644.
[33] W.U. Huynh, J.J. Dittmer, A.P. Alivisatos, Science 295 (2002) 2425–2427.
[34] Z.E. Ooi, T.L. Tam, R.Y.C. Shin, Z.K. Chen, T. Kietzke, A. Sellinger, M. Baumgarten, K. Mullen, J.C. deMello, J. Mater. Chem. 18 (2008) 4619–4622.
[35] I. Gur, N.A. Fromer, M.L. Geier, A.P. Alivisatos, Science 310 (2005) 462–465.
[36] J.B. Cui, U.J. Gibson, J. Phys. Chem. B 109 (2005) 22074–22077.
[37] J. Datta, C. Bhattacharya, S. Bandyopadhyay, Appl. Surf. Sci. 253 (2006) 2289–2295.
[38] P.J. Kulesza, J.A. Cox, Electroanalysis 10 (1998) 73–80.
[39] M. Jakič, M. kovač, K. Gaberšček, S. Pejovnik, Electrochim. Acta 40 (1995) 2723–2729.
[40] P.K. Biswas, A. De, L.K. Dua, L. Chkoda, Appl. Surf. Sci. 253 (2006) 1953–1959.
[41] S. Janietz, D.D.C. Bradley, M. Grell, C. Giebeler, M. Inbasekaran, E.P. Woo, Appl. Phys. Lett. 73 (1998) 2453–2455.
[42] R. Valaski, C.D. Canestraro, L. Micaroni, R.M.Q. Mello, L.S. Roman, Sol. Energy Mater. Sol. Cells 91 (2007) 684–688.
[43] C.F. Klingshrin, Semiconductor Optics, Springer-Verlag, Berlin, 1997.
[44] V. Srikant, D.R. Clarke, J. Appl. Phys. 81 (1997) 6357–6364.
[45] C. Baban, G.I. Rusu, Appl. Surf. Sci. 211 (2003) 6–12.
[46] J.C. Jernigan, W. Murray Royce, J. Am. Chem. Soc. 109 (1987) 1738–1745.
[47] Klaus Schwarzburg, Ralph Ernstorfer, Silke Felber, Frank Willig, Coord. Chem. Rev. 248 (2004) 1259–1270.
[48] R. Tena-Zaera, T.A. Kattya, S. Bastide, C. Lévy-Clémenta, B. O'Regan, V. Muñoz-Sanjosé, Thin Solid Films 483 (2005) 372–377.
[49] G. Hodes, Adv. Mater. 19 (2007) 639–655.
[50] R. Tena-Zaera, M.A. Ryan, A. Katty, G. Hodes, S. Bastide, C. Lévy-Clément, C. R. Chimie 9 (2006) 717–729.
[51] M. Nanu, J. Schoonman, A. Goossens, Adv. Mater. 16 (2004) 453–456.
[52] C. Lévy-Clément, R. Tena-Zaera, M.A. Ryan, A. Katty, G. Hodes, Adv. Mater. 17 (2005) 1512–1515.
[53] H.W. Deckman, C.R. Wronski, H. Witzke, E. Yablonovitch, Appl. Phys. Lett. 42 (1983) 968–970.